

Hybrid Watermarking Scheme for Halftone Images

Ching-Tang Hsieh, Yeh-Kuang Wu, and Kuo-Ming Hung¹

Dep. of Electrical Engineering, Tamkang University, Taiwan
¹ Dep. of Information Management, Kainan University, Taiwan

121590@mail.tku.edu.tw

Abstract. As digital halftone images are widely used in the printing of books, magazines, newspapers and computer printers, the ease with which perfect copies can be made, may lead to large-scale unauthorized copying. Watermarking has been considered for many copy prevention and copyright protection applications. The hybrid watermarking system is proposed for halftone images that the watermarks embedded based on the spatial domain and frequency domain separately to enhance the robustness. For the purpose of copyright protection, the watermarks are embedded into the halftone image with visual transparency and robustness by the variety of dispersed dot order dither arrays generated by the particle swarm optimization (PSO) method achieving good robustness and image quality produce patterns for the spatial watermarks embedding system. After the binary pseudo-wavelet transform (BPWT), the second watermarks are embedded into the high-frequency components of the BPWT coefficients of the spatial domain based watermarked image that the frequency domain based watermarking is independent to the spatial domain based one. And the modified quality criterion system for halftone images is proposed by using the PSO based visual filter. The experimental results show that the hybrid watermarking algorithm is more robust for halftone images and the watermarked halftone image possesses high image quality by the PSO algorithm.

Keywords: Watermark, Halftone Image, PSO,

1 Introduction

Digital halftone images are widely used in the printing of books, newspapers and computer printers. Halftone images contain only two tones and are generated by a procedure called halftoning from multi-tones images. Printing or displaying images on limited bit-depth devices is a crucial step, and several kinds of halftoning methods were published, including order dithering, error diffusion, dot diffusion, and least square error. However, owing to advances in digital technologies, most data are digitized and can be easily copied or edited. Such a situation hinders the popularization of digital technologies. Digital watermarking provides a solution for protecting the copyright of digital contents [1-3]. Several watermarking methods for halftone images have been proposed [4-6]. Fu et al. [7][8] embedded a single watermark or multi-watermarks in the parity domain of halftone images during

half-toning, but the finite number of watermarks is not enough for copyright authentication. Fu et al. [9-12] also proposed the data hiding by modified stochastic error diffusion to embed a binary hidden visual pattern in two diffused halftone images. However, the host image is essential in the watermark extracting procedure, and this proposal is not suitable for practical application. Pei et al. [13] proposed a technique by embedding the robust watermark into a dithered image after the pre-process of bit-interleaving and sub-image-interleaving to maintain low computational complexity of ordered dithering. The watermarked halftone image by Pei's method has higher visual quality with low capacity. But it is not robust to malicious attacks and geometric distortion. In Hagit's work [14], the watermark is embedded in the printed images by using a number of different dither cells to create a threshold pattern. But, it is not robust to cropping and contains low transparency.

Other hybrid watermarking systems hide information into the host images based on spatial and frequency domain simultaneously [15][16]. To enhance the robustness of watermarking system, some hybrid watermarking system had been noticed, but it is difficult for the hybrid watermarking for halftone images since the system should maintain the independence between these two watermarks and reduce the effect of the latter embedded watermarks on the former ones, and it is also difficult to design the watermarking system for halftone images based on frequency domain such as the wavelet transform or cosine transform since of the only two tones that halftone images containing.

Pigeon [17] proposed the binary pseudo-wavelets transform (BPWT) based on the binary domain that exhibits some of the properties of wavelets, such as localization in space and multi-resolution reconstruction transforming the image into the frequency domain. Furthermore, binary pseudo-wavelets are computed using only the logical operation, "and" and "or".

Here, a novel hybrid watermarking system is proposed for halftone images achieving the goal of copyright protection by embedding robust watermarks based on spatial and frequency domain separately. Authors had proposed the optimized watermarking embedding system based on the particle swarm optimization (PSO) [22] generating the optimized dither cells pair mapped to watermarks. In the method, the optimized dither cell is adopted to enhance the quality and robustness of the watermarked halftone image. Then the watermarked halftone images are transformed to frequency domain by the BPWT, and the other watermarks would be also embedded in the high-frequency components of BPWT coefficients as frequency domain based watermarking. Finally, the modified quality criterion system for halftone images is proposed by using the PSO based visual filter.

In section 2 and 3, we will describe the dithering technique in halftone images and the binary pseudo-wavelet transform. And the proposed multi-purpose watermarking system in halftone images is shown in section 4. The experimental results and the evaluation of the proposed algorithm are presented in section 5. Finally, section 6 shows the conclusion.

2 Halftoning Using Dithering

The digital halftoning methods can be divided into two main categories: ordered dithering and error diffusion [2]. The error diffusion method has higher computational complexity but can obtain a higher quality. The order dithering is the easier method to be implemented because it does not require processing or storage of neighboring pixels. In the order dithering, pixels from the input images are compared with the elements of the dither cell, and the halftone image H is defined by (1). The original image is denoted by I , respectively (x,y) . The halftone image $H(x,y)$ is defined by (1), where the dither cell $T(x,y)$ is the dither cell.

$$H(x,y) = \begin{cases} 1 & \text{if } I(x,y) > T(x,y) \\ 0 & \text{if } I(x,y) \leq T(x,y) \end{cases} \tag{1}$$

3. Binary Pseudo-wavelets Transform

Pigeon proposed the binary pseudo-wavelets transform (BPWT) based on the binary domain exhibiting some of the properties of wavelets, such as localization in space and multi-resolution reconstruction and transform the image into the frequency domain. It also provides means to lossy compression with graceful degradation of the image. Furthermore, binary pseudo-wavelets are computed using only the logical operation, “and” and “or” whereas classical wavelets require more or less complex arithmetic operations to compute the transforms. Table1 shows the binary pseudo-wavelet basis W and its inverse W^{-1} .

$$C = W \times (W \times I)^T \tag{2}$$

$$\bar{I} = W^{-1} \times (W^{-1} \times C)^T \tag{3}$$

where I is the image of the halftone images and C is the image after BPWT processing. \bar{I} is the image of the inverse BPWT.

Fig. 2 shows the position labelling of BPWT coefficients and its characteristics. The components at the right-down side are the low-frequency components, and the high-frequency components are located at the left-up side.

$$W = \begin{bmatrix} 1 & 0 & 0 & 0 & 1 & 0 & 1 & 0 \\ 1 & 0 & 0 & 0 & 0 & 0 & 0 & 0 \\ 0 & 1 & 0 & 0 & 1 & 0 & 0 & 0 \\ 0 & 1 & 0 & 0 & 0 & 0 & 0 & 0 \\ 0 & 0 & 1 & 0 & 0 & 1 & 0 & 1 \\ 0 & 0 & 1 & 0 & 0 & 0 & 0 & 0 \\ 0 & 0 & 0 & 1 & 0 & 1 & 0 & 0 \\ 0 & 0 & 0 & 1 & 0 & 0 & 0 & 0 \end{bmatrix} \quad W^{-1} = \begin{bmatrix} 1 & 1 & 1 & 1 & 0 & 0 & 0 & 0 \\ 0 & 0 & 0 & 0 & 1 & 1 & 1 & 1 \\ 1 & 1 & 0 & 0 & 0 & 0 & 0 & 0 \\ 0 & 0 & 0 & 0 & 1 & 1 & 0 & 0 \\ 1 & 0 & 0 & 0 & 0 & 0 & 0 & 0 \\ 0 & 0 & 1 & 0 & 0 & 0 & 0 & 0 \\ 0 & 0 & 0 & 0 & 1 & 0 & 0 & 0 \\ 0 & 0 & 0 & 0 & 0 & 0 & 1 & 0 \end{bmatrix}$$

Fig. 1. Binary pseudowavelet basis and its inverse basis.

4. Proposed Watermarking Methods

The flowcharts of proposed hybrid watermark embedding and extracting systems are shown in Fig. 2 and Fig. 3 respectively. Two different dither cells, C_0 and C_1 , optimized generating by PSO [22], are adopted and will be selected according to the watermark as the watermark embedding system. The image is divided into several blocks image with size $N \times N$ pixels. The two different cells should produce different halftone patterns according to the embedding watermarks. The watermark is a binary watermark $w = \{w^0, w^1 \dots w^{M_w \times N_w}\}$ which size is $M_w \times N_w$ pixels. The watermark will be coded by the 4 times repetition coding as ECC coding and random permuting, and the size of embedding watermark is $4M_w \times 4N_w$ pixels. In the chapter, the size of sub-blocks would be set to 8×8 pixels. The test image is the gray level image with size 512×512 pixels.

4.1 Watermark Embedding

In each sub-image, alternative dither cells will be selected according to the watermarks w . The procedures of robust watermarks embedding system is given in detail as follows:

1. The host image I is segmented into n sub-images that the size is $N \times N$ pixels.
2. For each sub-image I^n , the cell C_0 is adopted to be the dither cell when the corresponding robust watermark is "0". Cell C_1 will be selected when the corresponding robust watermark is "1".
3. Halftone the sub-image by the (1) with the dither cell T , C_0 or C_1 , selected by step 2. And get the halftone sub-image H^n .

In the system, the robust watermarks are embedded in all points of the image. However, the watermarking system described above is not robust to scaling attack. If other watermarks are embedded into the image above robust watermarks to enhance the robustness, it will affect the robustness of former robust watermarks.

Here, the hybrid watermarking system is proposed that another watermark is embedded based on the frequency domain which is independent to the spatial watermarking system described above. In the first step, the sub-block image is transformed into the frequency domain by the BPWT and denoted as H_{BW}^n . For each block n , the watermarks will be embedded into the higher frequency BPWT coefficient of the halftone image with robust watermarks. The equation is shown as follows.

$$H_{BW}^n(62) = \begin{cases} 0, & \text{if } w^n = 0 \\ 1, & \text{if } w^n = 1 \end{cases} \quad (4)$$

After the inverse BPWT, the n th hybrid watermarked halftone sub-image H_{Hy}^n containing both spatial domain based watermarks and frequency domain ones would be obtained.

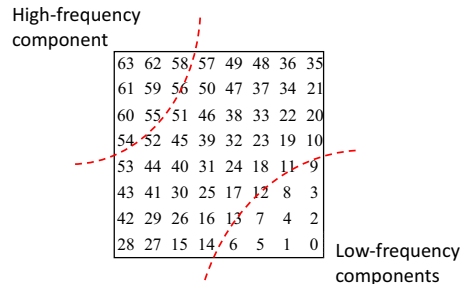


Fig. 2. Labeling positions of the BPWT coefficients.

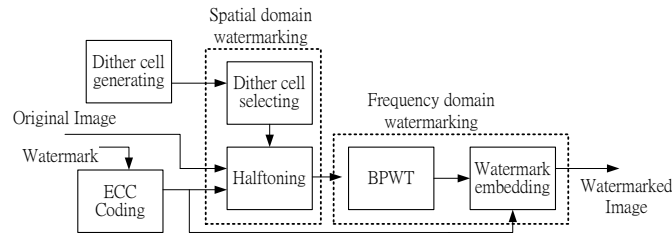


Fig. 3. Proposed watermark embedding system.

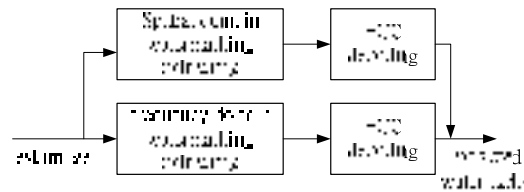


Fig. 4 Proposed watermarks extracting system.

4.2 Watermark Extracting

The watermarked halftone image is segmented into n th sub-images \bar{H}_{Hy}^n with size $N \times N$ pixels. The reference sub-images, $H_{C_0}^n$ and $H_{C_1}^n$, similar to the original halftone sub-image will be selected as the decoding dither cells and the corresponding watermark bits could be extracted. The two reference sub-images are generated by the dither cells C_0 and C_1 .

$$H_{C_0}^n(x, y) = \begin{cases} 1, & C_0(x, y) < \bar{H}_{Hy_MEAN}^n \\ 0, & C_0(x, y) \geq \bar{H}_{Hy_MEAN}^n \end{cases} \quad (5)$$

$$H_{C_1}^n(x, y) = \begin{cases} 1, & C_1(x, y) < \bar{H}_{Hy_MEAN}^n \\ 0, & C_1(x, y) \geq \bar{H}_{Hy_MEAN}^n \end{cases} \quad (6)$$

$$\bar{H}_{Hy_MEAN}^n = \sum_{y=1}^N \sum_{x=1}^N \bar{H}_{Hy}^n(x, y) / 255 \tag{7}$$

$$\bar{w}_{Spt}^n = \begin{cases} 1, & \sum_{x=1}^N \sum_{y=1}^N |H_{C_1}^n(x, y) - \bar{H}_{Hy}^n(x, y)| < \sum_{x=1}^N \sum_{y=1}^N |H_{C_0}^n(x, y) - \bar{H}_{Hy}^n(x, y)| \\ 0, & otherwise \end{cases} \tag{8}$$

$\bar{H}_{Hy_MEAN}^n$ is the number of the white points in the n th sub-images. If the halftone region generated by dither cell C_1 is more similar than the region generated by dither cell C_0 , the extracted robust watermark is set to 1. And if the halftone region generated by dither cell C_0 is more similar, the extracted robust watermark is set to 0.

The steps of robust watermark extracting procedure are described as follows:

1. For each sub-image n , calculate the number of white points in each block by (7).
2. Compute two reference halftone sub-images $H_{C_0}^n$ and $H_{C_1}^n$ by (5) and (6).
3. Extract the dither cell and its corresponding watermark (8).
4. De-permute and extract the watermark by ECC decoding.

After the spatial domain based watermarks extraction, the watermarks embedded based on the frequency domain would be extracted. For each sub-image n , after the BPWT, the frequency domain based watermarks are extracted from the high-frequency components of BPWT coefficients.

5. For each sub-image n , after the BPWT, extract the highest frequency components denoted as $\bar{H}_{HyBW}^n(63)$.
6. Extract watermark \bar{w}_{freq}^n by the following equation.

$$\bar{w}_{freq}^n = \begin{cases} 1, & \text{if } \bar{H}_{HyBW}^n(63) = 1 \\ 0, & \text{if } \bar{H}_{HyBW}^n(63) = 0 \end{cases} \tag{9}$$

4.3 Quality Criterion by PSO

The quality criterion of the visually image quality is defined as

$$PSNR = 10 \log_{10} \frac{255^2}{MSE} \tag{10}$$

$$MSE = \frac{1}{PQ} \sum_{i=1}^P \sum_{j=1}^q (org(i, j) - emb(i, j))^2 \tag{11}$$

where MSE is the mean square error of the image, org_i is the coefficient of the original image in position (i, j) , respectively; emb is the embedded image. However, the WPSNR value for measuring the quality of images is suitable gray level images, not for the halftone images. The WPSNR for halftone image is given as follow:

$$WPSNR = 10 \log_{10} \frac{255^2}{MSE} \tag{12}$$

$$MSE = \frac{1}{PQ} \sum_{i=1}^P \sum_{j=1}^q (org(i, j) - \sum_{u,v \in R} \sum w(u, v) H(i + u, j + v)) \quad (13)$$

where $H(i, j)$ is the corresponding halftone image in position (i, j) , respectively; $w(u, v)$ is the human visual coefficient at (u, v) and R is the support region of the human visual coefficients. [24] proposes the MPSNR to measure the perceptual quality of the halftone images that the w is the Gaussian lowpass filter. The other method [13], WPSNR, obtains w is to using the training set Least-Mean-Square (LMS).

However, the optimum human visual filter generated by LMS would be obtained by the extensive computation and cost lots of time. The PSO based human visual coefficients is proposed in the method. PSO algorithm is an evolutionary computation technique developed by Eberhart and Kennedy [23] in 1995, which was inspired by the social behavior of bird flocking and fish schooling, and is effective in optimizing difficult multidimensional discontinuous problems in a variety of fields. These particles fly through hyperspace and have two essential reasoning capabilities: their memory of their own best position and knowledge of their neighborhood's best.

The position of each particle is used to compute the value of the fitness function to be optimized. Eight images are adopted as the training image such as Lena, Mandrill, Peppers, Milks, Airplane, Earth, Lake and Tiffany, and three halftoning methods, error diffusion, Bayer-5 and Classical-4, are included. The algorithm of the PSO based human visual filter is given as follows:

Initialization

The particle dimension is $N_G \times N_G$ and particle number is set to 20, with N_G set to 7 is the method. In the particle swarm optimization algorithm, the initial value of each particle is an essential stage since the good initial value will speed up the time of convergence and increase the accuracy. In our method, the elements of each particle are Gaussian distribution with random standard deviation.

Fitness calculation

In the method, the image quality of the halftone image will be adopted as the fitness function and defined as follows.

$$PPSNR_i = 10 \log_{10} \frac{255^2}{MSE} \quad (14)$$

$$MSE = \frac{1}{PQ} \sum_{i=1}^P \sum_{j=1}^q (org(i, j) - \sum_{u,v \in R} \sum P_i^n(u, v) H(i + u, j + v)) \quad (15)$$

where P_i^n is the i th particle at the n stage. $PPSNR_i$ is the PSNR value of the particle i .

Table 1 Visual quality simulate by different human visual filter's size.

Human visual filter's size	5 × 5	7 × 7	9 × 9
PPSNR	26.90	27.89	27.91

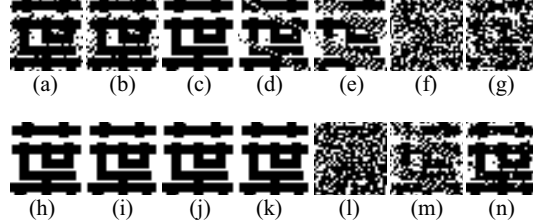


Fig. 5. Extracted spatial domain based watermarks under malicious attacks.

Compensation

The equation of compensation is shown as follows.

$$V_i^{n+1} = V_i^n + c_1 \times rand \times (pbest_i - WPSNR_i) + c_2 \times rand \times (gbest_i - WPSNR_i) \quad (16)$$

$$P_i^{n+1} = \mu P_i^n + V_i^{n+1} \quad (17)$$

Repetition

The process is repeated starting at stage (b) until the stopping or the iteration number is reached. And output the best result of the human visual filter w .

Table 1 shows the average PPSNR tested using the eight images listed above with various combinations of PSO based human visual filter size. Filter sizes of 9×9 or larger offer only a small improvement in quality, but substantially increase computational complexity. Therefore, the filter of size 7×7 offering a higher halftone quality is suitable to reconstruct the halftone image.

5. Simulations

The tested image is the grey level image with size 512×512 pixels in our experiments. The size of robust watermark is 32×32 pixels. In the simulation, the PPSNR is used to measure the perceptual quality of the halftone images. The PPSNR value of the watermarked images by the proposed spatial and frequency domain based watermarking system is given in Table 4.3. Note that the image quality of the watermarked halftone image containing dual spatial and frequency domain watermarks is still well even the spatial watermark capacity is 4096 bits. Table 3 shows the visual quality simulation based on different low-pass filters. PPSNR is the proposed method obtaining the human visual filter by PSO. WPSNR has the human visual filter by the LMS and the other one is obtained by Gaussian filter. The size of the human visual filter is 7×7 . In the table, PPSNR by the proposed method is higher than other ones.

Table 2 Image quality of watermarked halftone image by the proposed spatial domain based and frequency domain based watermarking systems

Capacity	Proposed spatial domain based watermarking system	Proposed hybrid watermarking system
Baseline	27.875	27.875
1024 bits	27.767	27.510
2048 bits	27.737	27.171
4096 bits	27.673	26.784

Table 3 Visual quality simulate by different human visual filter.

Human visual filter	PPSNR	WPSNR	MPSNR
	27.88	27.77	27.4668

Here, we present some image distortions and attacks for simulation shown as follows.

- (a) Cropping 25 %
- (b) Drawing in Black 25 %
- (c) Rotating 15 degree
- (d) Rotating 30 degree
- (e) Rotating 45 degree
- (f) Scaling (50%)
- (g) Scaling (75%)
- (h) Scaling (200%)
- (i) Pepper & Salt noise (20%)
- (j) Pepper & Salt noise (30%)
- (k) Pepper & Salt noise (40%)
- (l) Pepper & Salt noise (50%)
- (m) Pepper & Salt noise (60%)
- (n) Print and Scan

We measure the performance of watermarking system by the value of *Correct DR* defined as follows:

$$Correct\ DR = \frac{\sum_{i=1}^{M_w} \sum_{j=1}^{N_w} Xnor(org_w - new_w)}{M_w \times N_w} \quad (18)$$

where org_w is original watermark, new_w is the extracted watermark, and $Xnor$ is the Exclusive-Nor operator. Fig. 5 shows the extracted spatial domain based watermarks under different attacks. Fig. 6 shows the frequency domain based ones. And Table 4 shows the *Correct DR* value of the extracted spatial and frequency based watermarks. The capacity of watermark embedding in this simulation is 4096 bits in spatial domain watermarking and 3072 bits in frequency domain watermarking. In (f), the extracted spatial domain based watermarks from the tested image is under the scaling attack of the factor 0.5. The image quality is not good because of the non-

integral scaling factor and interpolation procedure. But the *Correct DR* of extracted frequency domain watermarks in (f) is high. In the attacks (a), (b), (d), (e) and (f), the *Correct DR* of the extracted frequency domain watermarks is better than the spatial domain. And in other attacks, the *Correct DR* of the extracted spatial domain watermarks is better than the frequency domain. Fig. 7 shows the *Correct DR* of the extracted spatial and frequency domain based watermarks and the hybrid system is a complementary system and the one of the extracted watermarks with higher decoding rate from the hybrid watermarking scheme would be selected as the final watermark. It is obvious that the proposed method with spatial domain based watermarking and frequency domain based watermarking is robust to malicious attacks such as scaling and rotation.

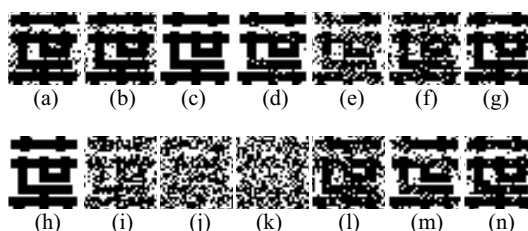


Fig. 6. Extracted frequency domain based watermarks under malicious attacks.

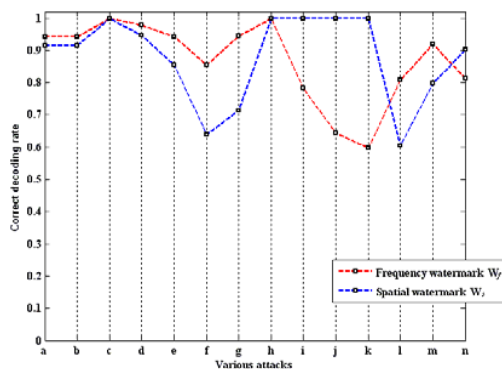


Fig. 7. *Correct DR* of extracted spatial and frequency domain based watermarks under malicious attacks.

Table 4 Visual quality comparisons measured by PPSNR.

Capacity	Methods	Lena	Baboon	Pepper
4096 bits	Proposed method using PSO based dither cell	27.89	27.39	27.78
4096 bits	Proposed method using Hagit's [45] dither cell	27.65	26.96	27.49
4096 bits	DHSPT[78]	26.58	26.50	26.73
4096 bits	BOPC[79]	26.77	26.58	26.84

The capacity and the visual quality of the watermarked images by the proposed method and by the Hagit's method are listed in Table 4. The Hagit's method emphasizes the capability of visual transparency. In the Table 4, the visual quality of watermarked images by our method is better than by the Hagit's method because the dither cell obtained by the PSO algorithm possesses the visual transparency and robustness.

6. Conclusions

In this chapter, we proposed the hybrid watermarking system for halftone images. According to dithered method, the robust spatial domain based watermarks are embedded by alternation dither cells pairs optimized by PSO algorithm. And the frequency domain based watermarks are embedded by the BPWT algorithm that the two watermarking systems are independent and complement. And modified quality criterion system for halftone images is proposed by the PSO-based human visual filter. From the experimental results, it is shown that the proposed hybrid method is a complementary system and is more robust to malicious attacks such as cropping and scaling. The watermarked image possesses high visual quality and is robust to malicious attacks.

References

1. Hartung, F., Kutter, M.: Multimedia watermarking techniques, Proc. of IEEE, Digital Object Identifier, vol. 87, pp. 1079–1107(1999).
2. Cox, I. J., Kilian, J., Leighton, F. T., Shamoon, T.: Secure spread spectrum watermarking for multimedia, Trans. on IEEE Image Processing, vol. 6, pp. 1673–1687(1997).
3. Hsieh, C.T., Wu, Y.K., Chen, H.Y.: Semi-fragile Image authentication using real-symmetric matrix, J. of Information Science and Engineering, vol. 22, pp. 701–712(2006).
4. Wang, P. W., Memon, N. D.: Image processing for halftones, IEEE Signal Processing Magazine, pp. 59–70(2003).
5. Ulichney, R.: The void-and-cluster method for dither array generation, Proc. of SPIE, pp. 332–343(2004).
6. Ulichney, R.: Digital Halftoning, The MIT Press. (1987).
7. Fu, M. S., Au, O.C.: A robust public watermark for halftone images, Proc. Circuits and Systems, vol. 3, pp. 639–642(2002).
8. Fu, M. S., Au, O.C.: A multi-bit robust watermark for halftone images," in Proc. Multimedia and Expo, vol. 1, pp. 213–216(2003).
9. Fu, M. S., Au, O.C.: Data hiding in halftone images by stochastic error diffusion," in Proc. Acoustics, Speech, and Signal Processing, vol. 3, 2001, pp. 1965–1968.
10. Fu, M. S., Au, O.C.: A novel self-conjugate halftone image watermarking technique," Proc. Circuits and System, vol. 3, pp. 790–793(2003).
11. Fu, M. S., Au, O.C.: A novel method to embed watermark in different halftone images: data hiding by conjugate error diffusion (DHCED)," Proc. Multimedia and Expo, vol. 1, pp. 609–612(2003).
12. Fu, M. S., Au, O.C.: A set of mutually watermarked halftone images, Proc. Image

- Processing, vol. 2, pp. 467 – 470(2003).
13. Pei, S.C., Guo, J.M., Lee, H.: Novel robust watermarking technique in dithering halftone images, *IEEE Letter on Signal Processing*, vol. 12, pp. 333–336(2005).
 14. Hagit, Z. H.-O.: Copyright labeling of printed images, *Proc. Image Processing*, vol.3, pp. 702–705(2000).
 15. Lu, C. S., Liao, L. Y. Mark: Multipurpose watermarking for image authentication and protection, *Trans. on IEEE Image Processing*, vol. 10, pp. 1579–1592(2001).
 16. Chen, T., Wang, J., Zhou, Y.: Combined Digital Signature and Digital Watermark Scheme for Image Authentication, *Proc. Info-tech and Info-net*, pp. 78–82(2001).
 17. Pigeon, S., Bengio, Y.: Binary Pseudowavelets and Applications to Bilevel Image Processing, *Proc. Data Compression Conference*, pp. 364–373(1999).
 18. Kennedy, J., Eberhart, R.C.: Particle swarm optimization, in *Proc. IEEE Neural Networks*, pp. 1942–1948(1995).
 19. Hsieh C.T., Wu, Y.K.: Geometric invariant semi-fragile Image authentication using real-symmetric matrix, *Trans. WSEAS on Signal Processing*, vol.5, pp.612–617(2006).
 20. Fu, M. S., Au, O. C.: Data Hiding Watermarking for Halftone Images, *IEEE Trans. on Images Processing*, vol. 11, No.4, pp.477–484(2002).
 21. Li, R. Y., Au, O. C.: Halftone Image Data Hiding with Block-Overlapping Parity Check, *Proc. ICASSP*, vol. 2, pp.193–196(2007).
 22. Hsieh, C.T., Wu, Y.K., Chung, W.Z.: Digital watermarking system for halftone images based on particle swarm optimization, *Proc. IEEE Conf. on Ubi-Media Computing*, pp.201–206, 2008.
 23. Kennedy, J., Eberhart, R.C.: Particle swarm optimization, *Proc. of IEEE Neural Networks*, pp. 1942–1948(1995).
 24. Sherry, P., Savakis, A.: Improved Techniques for Watermarking Halftone Images, *Proc. Acoustics, Speech, and Signal Processing*, vol. 5, pp.1005–1008(2004).